ISSN 0023-1584, Kinetics and Catalysis, 2022, Vol. 63, No. 2, pp. 166–171. © Pleiades Publishing, Ltd., 2022.
Russian Text © The Author(s), 2022, published in Kinetika i Kataliz, 2022, Vol. 63, No. 2, pp. 187–192.

Estimation of the Integral Toxicity of Photocatalysts Based on Graphitic Carbon Nitride in a Luminescent Test

E. B. Chubenko[a, *], A. V. Baglov[a], N. V. Dudchik[c], E. V. Drozdova[c], O. A. Yemelyanova[c], and V. E. Borisenko[a, b]

[a] *Belarusian State University of Informatics and Radioelectronics, Minsk, 220013 Belarus*
[b] *National Research Nuclear University MEPhI, Moscow, 115409 Russia*
[c] *Scientific Practical Centre of Hygiene, Minsk, 220012 Belarus*
** e-mail: eugene.chubenko@gmail.com*

Received May 18, 2021; revised July 19, 2021; accepted August 19, 2021

Abstract—A ternary heterosystem consisting of crystalline graphitic carbon nitride, zinc oxide, and zinc sulfide (g-C_3N_4/ZnO/ZnS) was obtained by the one-stage decomposition of a mixture of thiourea and zinc acetate. The integral toxicity index of the resulting material was estimated in a luminescent test with a genetically modified *Escherichia coli* strain as a test object. The effect of quenching the luminescence of *E. coli* was noted both under exposure to UV radiation due to photocatalytic reactions on the surface of g-C_3N_4/ZnO/ZnS leading to the formation of highly oxidative radical ions interacting with cell membranes and without irradiation due to mechanical interactions with bacterial cells. At a 0.3 g/L concentration of g-C_3N_4/ZnO/ZnS in aqueous solution, the toxicity index T reached 75.6% under UV irradiation. In this case, an increase in the toxicity index T of the ternary heterosystem in a test concentration range from 0.1 to 0.3 g/L was 6 or 10–11% under UV radiation or without illumination, respectively, as compared with that of the pure graphite-like carbon nitride obtained under identical conditions.

Keywords: graphitic carbon nitride, zinc oxide, zinc sulfide, nanoparticle, photocatalysis, *Escherichia coli*
DOI: 10.1134/S002315842202001X

INTRODUCTION

Clean drinking water is an important strategic resource for humanity because still a quarter of the world's population does not have currently constant access to it [1]. In addition to inorganic and organic particles and chemical compounds dissolved in water, various pathogenic microorganisms, such as bacteria, viruses, protozoa, and fungi, present in water are also dangerous [2, 3]. Conventional disinfection methods involve the use of chemicals containing chloride ions in most cases, and these ions are no less dangerous to humans than pathogenic microorganisms [3].

The use of photocatalytic reactions on the surface of semiconductors is an alternative disinfection method; these reactions lead to the appearance of highly reactive radical ions $OH^{\bullet}$, $O_2^{-\bullet}$, and $^1O_2$ and H_2O_2 molecules, which can interact with microorganisms to cause their death [4, 5]. The high efficiency of photocatalytic water purification was demonstrated using titanium oxide (TiO_2) [6, 7] and zinc oxide (ZnO) as photocatalysts [8, 9]. The large band gap and the position of the energy bands of these materials provide efficient heterogeneous photocatalysis, but the absorption spectrum of the above oxides narrows to the ultraviolet (UV) range, which is only 4% of the solar radiation energy [6–9]. Therefore, it is necessary to search for other materials with high photocatalytic activity that are easy to prepare and do not contain rare or expensive elements.

Graphitic carbon nitride (g-C_3N_4) is a unique organic semiconductor with a band gap of 2.70–2.88 eV at room temperature [10, 11], which has high chemical and thermal stability. It is recognized as an effective photocatalytic material, which can be used to generate hydrogen, purify water from chemical impurities, and disinfect it [10–12]. The structure of the material consists of monomolecular graphene-like layers of interconnected heptazine molecules held together by van der Waals forces; because of this, it is similar to the structure of graphite [10, 13]. In this regard, a similar mechanism of the action of g-C_3N_4 on pathogenic microorganisms can be expected, when the antibacterial effect is achieved due to both physical and chemical interactions [14–17]. Direct contacts of nanoparticles or individual monolayers of g-C_3N_4 with the protein membrane of a microorganism can lead to its mechanical damage and death of the organism due to leakage of the intracellular matrix. In addition, oxidative stress damages DNA and induces mitochondrial

dysfunction, which leads to the inhibition of bacterial reproduction and growth [18].

To increase the efficiency of g-C_3N_4 for water purification and disinfection, heterostructures including various wide-gap semiconductors, such as ZnO, TiO_2, ZrO_2, ZnS, SiC, or organic materials [19–23], which in themselves are also effective photocatalysts [24], are created on its basis. Multistep methods in which a g-C_3N_4 core is sequentially formed and covered with a wide-gap semiconductor shell are commonly used to obtain heterostructures based on g-C_3N_4.

In this work, we applied another principle for the creation of g-C_3N_4/wide-gap semiconductor heterostructures with the simultaneous pyrolytic decomposition of starting substances (precursors) and the in situ formation of a heterostructure using zinc acetate to obtain wide-gap zinc oxide and zinc sulfide particles in the heterostructure. We also evaluated the efficiency of these heterostructures for water purification to remove contaminating microorganisms in comparison with that of pure g-C_3N_4.

EXPERIMENTAL

Pure g-C_3N_4 was synthesized by the pyrolytic decomposition of precursors with their subsequent thermal polymerization as described previously [25, 26]. Thiourea was used as a precursor; a weighed portion of thiourea was placed in a ceramic crucible, which was then tightly closed with a massive lid through a gasket made of aluminum foil. This provided quasi-hermetic conditions under which excess gases could leave the crucible volume, but the penetration of substances from the outside was limited. The crucible prepared in this way was placed in a muffle furnace, heated to a target temperature of 500°C for 2 h, and kept for 30 min at this temperature. The crucible was gradually cooled for 8 h. The resulting material was removed from the crucible and mechanically crushed to a powdery state with a particle size of smaller than 10 μm.

The heterosystems based on graphitic carbon nitride, zinc oxide, and zinc sulfide were also synthesized by the pyrolytic decomposition of precursors with their subsequent thermal polymerization. In this case, thiourea and zinc acetate were used as starting compounds as described elsewhere [27, 28]. The portions of these substances of equal weights were placed in a ceramic crucible, tightly closed, and heated in a muffle furnace to a specified temperature of 500°C.

The structure and composition of the resulting materials were studied by scanning electron microscopy on an S-4200 electron microscope (Hitachi, Japan), X-ray microanalysis on a QUANTAX 200 spectrometer (Bruker, Germany), and X-ray diffractometry on a DRON-3 diffractometer (Russia) with a source of CuK_α radiation ($\lambda = 1.54179$ nm).

The toxic effect of a photocatalyst was evaluated using an Ecolum biosensor (Russia) based on a lyophilized culture of a specially selected genetically engineered strain of *Escherichia coli* (*E. coli*) luminescent bacteria with the lux operon embedded. The bacteria of the intestinal group are of sanitary significance, and they can contaminate water sources. Therefore, they are well suited as a model pollutant, which can be removed by a photocatalytic method.

The effect of photocatalysts on bacterial cultures was assessed using a Biotox-10M environmental monitoring instrument (NERA-S, Russia) by comparing the integral luminescence of samples containing bacteria in the presence of photocatalyst particles and reference samples without a photocatalyst. The toxicity index T, %, was determined as a percentage ratio between the difference of the luminescence intensities of the reference sample I_0 without the photocatalyst and the sample with the photocatalyst I_F and the luminescence intensity of the reference sample I_0:

$$T = 100 \times (I_0 - I_F)/I_0. \quad (1)$$

Before the measurements of the toxicity of samples, the Ecolum biosensor was rehydrated by adding 10 mL of sterile distilled water to a glass container with the biosensor and keeping the resulting suspension at room temperature for 30 min. Then, 0.1 mL of the working suspension of bacteria and 0.9 mL of a suspension of the powder particles of a test sample in distilled water were placed in the cells of the Biotox-10M environmental monitoring instrument. Instead, 0.9-mL portions of sterile distilled water were added to the reference samples. Thus, the total sample volume was 1 mL. The concentration of photocatalyst particles in the resulting samples was varied from 0.1 to 0.3 g/L. The toxicity of the samples was measured after 30 min of exposure. Some of the samples containing particles of materials based on carbon nitride were exposed to UV radiation for 30 min.

RESULTS AND DISCUSSION

A light yellow solid material with a complex microstructure, which included a large number of plates and particles ranging in size from 1 to 10 μm chaotically connected to each other was obtained as a result of the heat treatment of thiourea at 500°C in a closed crucible (Fig. 1a). According to X-ray microanalysis data, the synthesized material contained carbon and nitrogen in the ratio $C_C/C_N = 0.48$ (Table 1). This ratio is lower than the corresponding stoichiometric value (0.75) due to the incomplete polymerization of the material and a so-called kinetic limitation caused by the decomposition of the formed g-C_3N_4 with the release and evaporation of carbon-containing substances (in particular, HCN) in the course of the synthesis [17–19]. The oxygen concentration in the material was 5.43 at %.

The material obtained as a result of the heat treatment of a mixture of thiourea and zinc acetate was also yellowish brown solid powder, but it had a slightly different microstructure containing larger crystallites (Fig. 1b). The ratio of carbon to nitrogen was 0.82, which is higher than a stoichiometric value of 0.75. This fact indicates the presence of residual carbon, which can appear in the residual matter due to the decomposition of the acetate ion (CH_3COO^-) of zinc acetate in the closed volume of the crucible. The ratio C_{Zn}/C_S was 1.64, which exceeds the stoichiometric value of unity. The presence of excess zinc can be associated with oxygen, the concentration of which reached 7.45 at %. This value is 2 at % higher than the concentration of oxygen in the material formed upon the annealing of thiourea, and it is close to the amount of free zinc; this fact indicates the possibility of the occurrence of a ZnO phase.

The X-ray diffraction patterns of the samples (Fig. 2) showed lines corresponding to reflections from the (210), (002), and (600) crystallographic planes of g-C_3N_4 at the angles $2\theta = 12.75°$, 27.65°, and 44.45°, respectively [21]. The diffraction pattern of the sample synthesized from a mixture of thiourea and zinc acetate contained a large number of reflections from various crystallographic planes of ZnS with a cubic sphalerite-type crystal lattice and ZnO with a hexagonal lattice of the wurtzite type. The most intense peak at an angle of $2\theta = 27.5°$ corresponded to the (111) plane of ZnS, and the other peaks were related to reflections from the following planes: ZnS (200) at $2\theta = 33.2°$, ZnS (220) or ZnO (102) at 47.6°, ZnS (311) or ZnO (110) at 56.5°, ZnS (400) or ZnO (201) at 69.5°, and ZnS (331) or ZnO (202) at 76.9° [28].

Prokaryotic test models are well suited for evaluating biological action characteristics, integral toxicity, and antimicrobial potential in relation to innovative technologies and materials [6, 29–32]. The results of the evaluation of the integral toxicity of the obtained materials (Fig. 3) indicate that their destructive effects on opportunistic pathogens *E. coli* without exposure to UV radiation linearly increased in proportion to their concentration. The toxicity of particles synthesized from a mixture of thiourea and zinc acetate was, on average, 10–11% higher.

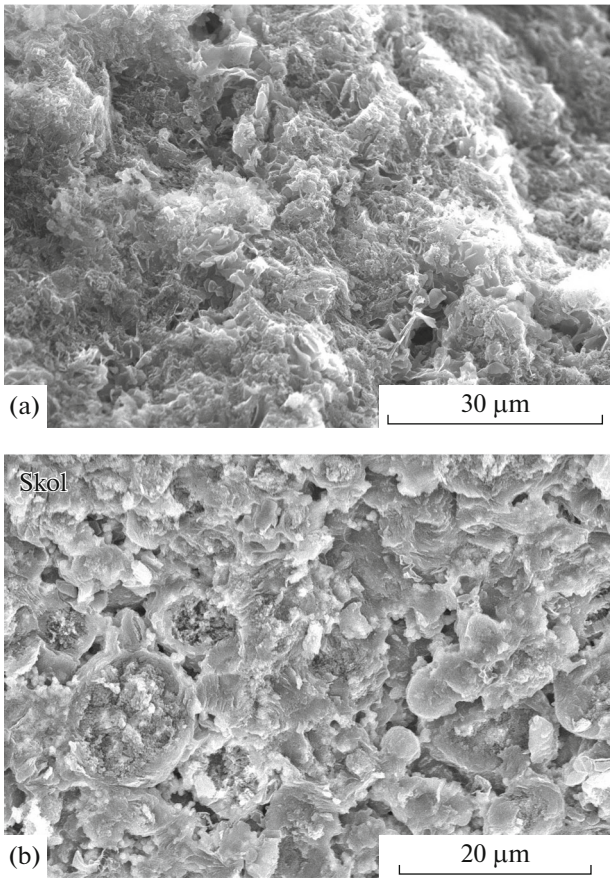

Fig. 1. Electron micrographs of the surfaces of (a) a powder obtained by the heat treatment of thiourea and (b) a thiourea/zinc acetate composite.

Irradiation with UV light led to an increase in the toxicity index T by 10–20% and a change in the dependence of its value on the concentration of the test materials in solution from linear to exponential. This value was higher than 50% at concentrations greater than 0.2 g/L; for this reason, the materials obtained can be classified as highly toxic substances.

Table 1. Elemental composition of the resulting materials

Precursor	Element concentration, at %					Element concentration ratio	
	C_C	C_N	C_O	C_{Zn}	C_S	C_C/C_N	C_{Zn}/C_S
Thiourea	30.80	63.77	5.43	–	–	0.48	–
Thiourea/zinc acetate	36.23	44.28	7.45	7.49	4.55	0.82	1.64

Dashes indicate the absence of the corresponding elements.

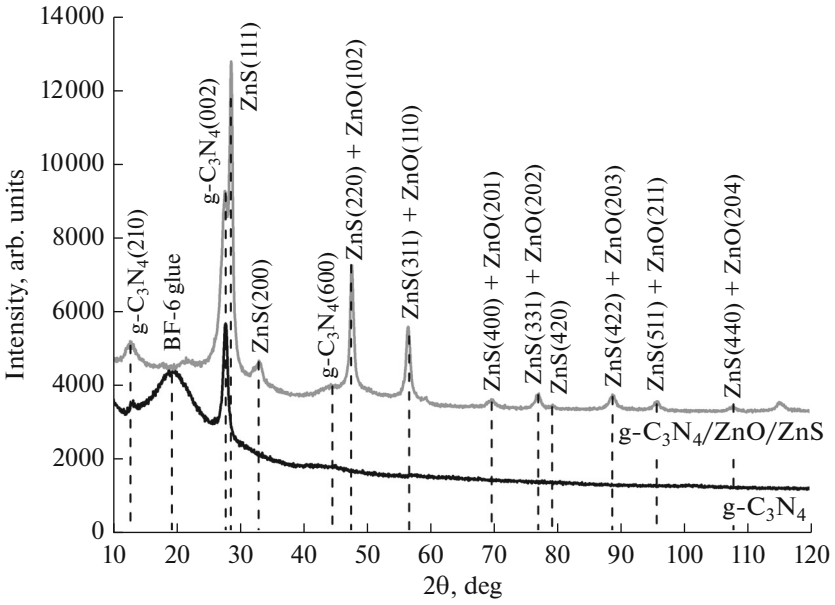

Fig. 2. X-ray diffraction patterns of a powder obtained by the heat treatment of thiourea and a thiourea/zinc acetate composite.

According to the results of X-ray microanalysis and X-ray diffractometry, the material synthesized as a result of pyrolytic decomposition of thiourea was polycrystalline bulk g-C_3N_4 with randomly located crystallites. The addition of zinc acetate to the starting reagents led to the formation of ZnS and ZnO crystals, which were embedded in a matrix of C_3N_4. Such a material can be designated as the ternary heterosystem g-C_3N_4/ZnO/ZnS. The formation of a ternary nanoheterosystem by the pyrolytic decomposition of thiourea and zinc acetate was described in detail elsewhere [27, 28]. In this process, the hydrogen sulfide formed as a result of the decomposition of thiourea reacts with zinc oxide, which is a decomposition product of zinc acetate, to form zinc sulfide under conditions of limited oxygen availability.

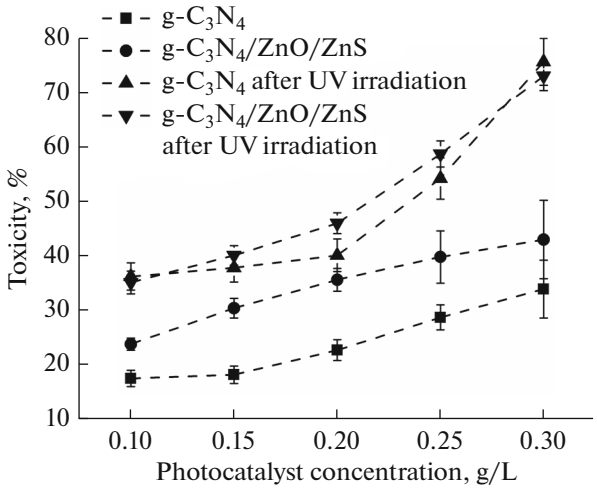

Fig. 3. Effects of the obtained materials on pathogenic microorganisms before and after exposure to UV radiation.

An increase in the toxicity of pure g-C_3N_4 particles with their concentration in solution without UV illumination showed that they exhibit a mechanical toxic effect, which is similar to that of graphene [14–16], on microorganisms leading to the destruction of their cell membranes upon direct contact. The demonstrated efficiency of the g-C_3N_4/ZnO/ZnS ternary heterosystem is higher due to an additional toxicological effect upon the direct contact of ZnO and ZnS nanoparticles with the protein shells of bacteria. In this contact, electron exchange can occur to induce the oxidative stress of microorganisms [33–35] or phosphate depletion of their membranes [33, 36].

Under UV irradiation, charge carriers are generated both in g-C_3N_4 and in ZnO and ZnS nanoparticles; then, they participate in the formation of hydroxyl radical ions $OH^{\bullet}$, superoxide ions $O_2^{-\bullet}$, and singlet oxygen $^1O_2$. Highly oxidizing ions react with bacterial cell membranes to cause their destruction, which leads to the observed increase in the toxic effects of pure g-C_3N_4 and the g-C_3N_4/ZnO/ZnS heterosystem.

The difference between the efficiencies of g-C_3N_4/ZnO/ZnS and pure g-C_3N_4 upon irradiation with UV light decreased in comparison with the results obtained in the absence of irradiation; however, the efficiency of the heterosystem remained somewhat higher. This fact indicates a more intense photocatalytic process involving both electrons and holes, which is achieved due to the wider band gaps of ZnO and

ZnS as compared to that of g-C_3N_4. However, pure g-C_3N_4 retained its high efficiency in water disinfection due to its large specific surface area.

CONCLUSIONS

The g-C_3N_4/ZnO/ZnS ternary heterosystem obtained in situ in a process using the thermal decomposition of thiourea and zinc acetate at a temperature of 500°C demonstrated photocatalytic efficiency to 75.6% under irradiation of microorganisms with UV light at a maximum test concentration of 0.3 g/L with the use of *E. coli* as an example. The photocatalytic effect of the g-C_3N_4/ZnO/ZnS heterosystem was somewhat higher than that of pure g-C_3N_4 obtained under identical conditions due to a heterogeneous photocatalytic process on the surface of crystals of the wide-band-gap semiconductors ZnO and ZnS.

The particles of pure g-C_3N_4 and the g-C_3N_4/ZnO/ZnS system also exhibit high toxicity without UV irradiation due to mechanical toxic effects on microorganisms leading to the destruction of their cell membranes upon direct contact. In this case, g-C_3N_4/ZnO/ZnS is more effective due to the toxicological effect of ZnO and ZnS nanoparticles in their direct contact with the protein shells of bacteria.

FUNDING

These studies were carried out within the framework of the State Research Program of the Republic of Belarus "Materials Science, New Materials, and Technologies" 1.4.

ACKNOWLEDGMENTS

We are grateful to D.V. Zhigulin for analyzing the structure of the samples by scanning electron microscopy and to Professor V.V. Uglov for performing the X-ray diffraction analysis of the samples.

CONFLICT OF INTEREST

The authors declare that they have no conflicts of interest.

REFERENCES

1. Zhang, C., Li, Y., Shuai, D., Shen, Y., Xiong, W., and Wang, L., *Chemosphere*, 2019, vol. 214, p. 462.
2. Drozdova, E.V., *Gig. Sanit.*, 2012, vol. 6, p. 78.
3. Li, Q., Mahendra, S., Lyon, D.Y., Brunet, L., Liga, M.V., Li, D., and Alvarez, P.J., *Water Res.*, 2008, vol. 42, p. 4591.
4. Wang, D., Pillai, S.C., Ho, S.H., Zeng, J., Li, Y., and Dionysiou, D.D., *Appl. Catal., B*, 2018, vol. 237, p. 721.
5. Wang, D., Zhu, B., He, X., Zhu, Z., Hutchins, G., Xu, P., and Wang, W.N., *Environ. Sci. Nano*, 2018, vol. 5, p. 1096.
6. Dudchik, N.V., Drozdova, E.V., and Sychik, S.I., *Health Risk Anal.*, 2018, vol. 3, p. 104–111.
7. Zhang, C., Li, Y., Wang, D., Zhang, W., Wang, Q., Wang, Y., and Wang, P., *Environ. Sci. Pollut. Res.*, 2015, vol. 22, p. 10444.
8. Lee, K.M., Lai, C.W., Ngai, K.S., and Juan, J.C., *Water Res.*, 2016, vol. 88, p. 428.
9. Spasiano, D., Marotta, R., Malato, S., Fernandez-Ibañez, P., and Di Somma, I., *Appl. Catal., B*, 2015, vols. 170–171, p. 90.
10. Wen, J., Xie, J., Chen, X., and Li, X., *Appl. Surf. Sci.*, 2017, vol. 391, p. 72.
11. Wang, A., Wang, C., Fu, L., Wong-Ng, W., and Lan, Y., *Nano-Micro Lett.*, 2017, vol. 9, p. 47.
12. Wang, X., Maeda, K., Thomas, A., Takanabe, K., Xin, G., Carlsson, J.M., Domen, K., and Antonietti, M., *Nat. Mater.*, 2009, vol. 8, p. 76.
13. Dong, F., Li, Y.H., Wang, Z.Y., and Ho, W.K., *Appl. Surf. Sci.*, 2015, vol. 358, p. 393.
14. Akhavan, O. and Ghaderi, E., *ACS Nano.*, 2010, vol. 4, p. 5731.
15. Li, X., Li, F., Gao, Z., and Fang, L., *Bull. Environ. Contam. Toxicol.*, 2015, vol. 95, p. 25.
16. Liu, S., Zeng, T.H., Hofmann, M., Burcombe, E., Wei, J., Jiang, R., Kong, J., and Chen, Y., *ACS Nano.*, 2011, vol. 5, p. 6971.
17. Wang, X., Liu, X., and Han, H., *Colloids Surf. B*, 2013, vol. 103, p. 136.
18. Zhao, J., Wang, Z., White, J.C., and Xing, B., *Environ. Sci. Technol.*, 2014, vol. 48, p. 9995.
19. Ong, W.J., Tan, L.L., Ng, Y.H., Yong, S.T., and Chai, S.P., *Chem. Rev.*, 2016, vol. 116, p. 7159.
20. Shi, L., Liang, L., Wang, F., Liu, M., Chen, K., Sun, K., Zhang, N., and Sun, J., *ACS Sustainable Chem. Eng.*, 2015, vol. 3, p. 3412.
21. Jürgens, B., Irran, E., Senker, J., Kroll, P., Müller, H., and Schnick, W., *J. Am. Chem. Soc.*, 2003, vol. 125, p. 10288.
22. Ismael, M., *J. Alloys Compd.*, 2020, vol. 846, p. 156446.
23. Liang, J., Yang, X., Wang, Y., He, P., Fu, H., Zhao, Y., Zou, Q., and An, X., *J. Mater. Chem. A*, 2021, vol. 9, p. 12898.
24. Vaizogullar, A.I., *Kinet. Catal.*, 2018, vol. 59, p. 418.
25. Chubenko, E.B., Denisov, N.M., Baglov, A.V., Bondarenko, V.P., Uglov, V.V., and Borisenko, V.E., *Cryst. Res. Technol.*, 2020, vol. 55, p. 1900163.
26. Baglov, A.V., Chubenko, E.B., Hnitsko, A.A., Borisenko, V.E., Malashevich, A.A., and Uglov, V.V., *Semiconductors*, 2020, vol. 54, p. 226.
27. Chubenko, E.B., Baglov, A.V., and Borisenko, V.E., *Adv. Photonics Res.*, 2020, vol. 1, p., 2000004.

28. Chubenko, E.B., Baglov, A.V., Leanenia, M.S., Urmanov, B.D., and Borisenko, V.E., *Mater. Sci. Eng., B*, 2021, vol. 267, p. 115109.

29. Dudchik, N.V., *Vestn. Ross. Voenno-Meditsinskoi akademii*, 2008, vol. 1, p. 148.

30. Dudchik, N.V., Filonov, V.P., and Shcherbinskaya, I.P., *Meditsinskii Zhurn.*, 2010, no. 3(33), p. 143.

31. Dudchik, N.V., Sychik, S.I., and Shevlyakov, V.V., *Theor. Appl. Ecology*, 2018, no. 4, p. 5.

32. Drozdova, E.V., Dudchik, N.V., Sychik, S.I., and Shevlyakov, V.V., *Otsenka integral'noi toksichnosti faktorov i ob"ektov sredy obitaniya s ispol'zovaniem al'ternativnykh biologicheskikh test-modelei: metodologiya i tekhnologii* (Evaluation of Integral Toxicity of Environmental Factors and Objects Using Alternative Biological Test Models: Methodology and Technologies), Minsk: BelNIIT "Transtekhnika," 2017, p. 212.

33. Leung, Y.H., Xu, X., Ma, A.P.Y., Liu, F., Ng, A.M.C., Shen, Z., Gethings, L.A., Guo, M.Y., Djurišić, A.B., Lee, P.K.H., Lee, H.K., Chan, W.K., and Leung, F.C.C., *Sci. Rep.*, 2016, vol. 6, p. 35243.

34. Li, J., Wang, G., Zhu, H., Zhang, M., Zheng, X., Di, Z., Liu, X., and Wang, X., *Sci. Rep.*, 2014, vol. 4, p. 4359.

35. Vecitis, C.D., Zodrow, K.R., Kang, S., and Elimelech, M., *ACS Nano*, 2010, vol. 4, p. 5471.

36. Gerber, L.C., Moser, N., Luechinger, N.A., Stark, W.J., and Grass, R.N., *Chem. Commun.*, 2012, vol. 48, p. 3869.

Translated by V. Makhlyarchuk